Chapter II

X-RAY DIFFRACTION METHODS

2.1 The Reciprocal Lattice[1]

The concept of the reciprocal lattice was first developed by Ewald. References to reciprocal-lattice theory are common in discussions of x-ray diffraction from crystals. The definition of the reciprocal lattice may be expressed as

$$d^*_{hkl} = \frac{K}{d_{hkl}}$$

where d^*_{hkl} is the distance from the origin to the reciprocal point corresponding to the family of planes having the spacing d_{hkl}, K is an arbitrary constant. Each reciprocal point represents a family of planes in the direct lattice.

From Bragg law :

$$\sin \theta_{hkl} = \frac{\lambda}{2d_{hkl}}$$

we can construct the reflecting sphere with unit radius; this sphere passes through the origin of the reciprocal lattice, O. The diameter XO is the direction of the x-ray beam through the origin. If a reciprocal point, P, lies on the surface of this sphere, then IP is the direction of the

---

[1]N.F.M Henry, H. Lipson, and W.A. Wooster, <u>The Interpretation of X-Ray Diffraction Photographs</u> (New York : Macmillan and Co., Ltd. 1961) p40.

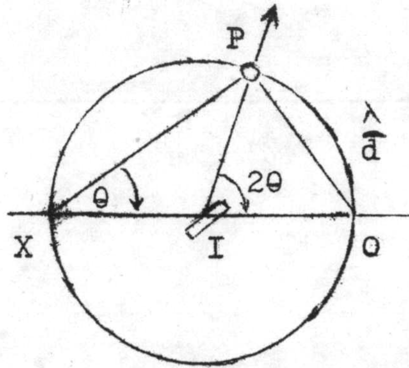

Fig.1 Sphere of reflection.

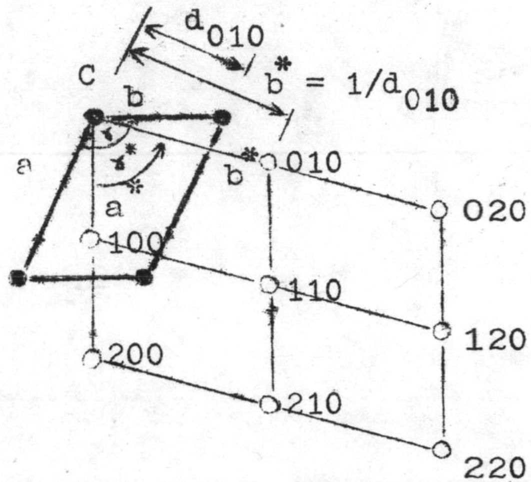

Fig.2 The relation between the direct lattice (heavy lines, solid circles) and the reciprocal lattice.

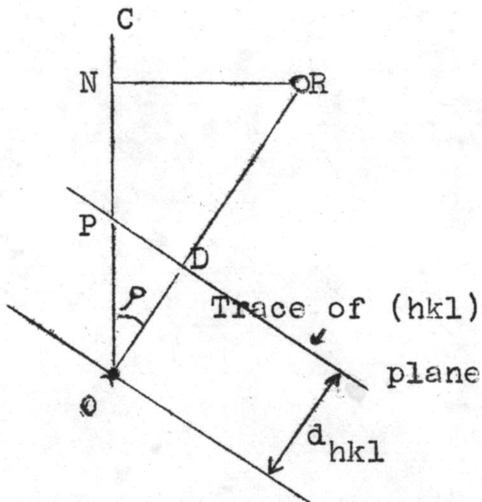

Fig.3 Formation of a lattice array by reciprocal points.

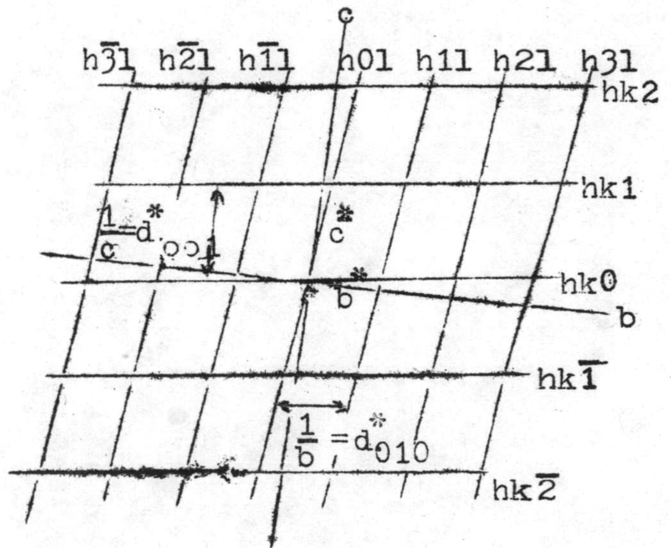

Fig.4 The relation between re- -ciprocal-lattice plane and direct-lattice rows.

reflected beam and PX is parallel to the planes corresponding to P and hence $P\hat{X}O = \theta$. Since $\sin\theta = \frac{OP}{OX} = \frac{\lambda}{2d}$ Bragg law is thus obeyed and these planes corresponding to P can reflect x-rays (Fig 1).

The relation between the space or direct lattice and the reciprocal lattice is shown in Fig.2. The direct lattice, identified by solid circles, is oriented in this diagram with the C-axis normal to the page; hence all (hko) planes are also normal to the page. Each plane of the direct lattice is represented by a point (open circles) that lies on the normal to the plane at a distance of $\frac{1}{d_{hkl}}$ from the origin. These points constitute the reciprocal lattice.

It follows from the concept of the reciprocal lattice that reciprocal rows are normal to planes of the direct lattice. The reciprocal lattice vector, $\vec{\sigma}_{hkl}$, can be expressed in terms of the direct lattice as[2]

$$\left|\vec{\sigma}_{hkl}\right| = \frac{1}{d_{hkl}},$$

and

$$\vec{\sigma}_{hkl} = h\bar{a}^* + k\bar{b}^* + l\bar{c}^*.$$

Three special cases of this relation are

$$a^* = \frac{1}{d_{100}},$$

$$b^* = \frac{1}{d_{010}},$$

---

[2] M.J. Buerger, X-Ray Crystallography (New York : John Wiley and Sons, 1953) pp 119-121

$$c^* = \frac{1}{d_{001}},$$

where a^*, b^*, and c^* are the unit translations of the reciprocal lattice.

Formation of a Lattice Array by Reciprocal Points

It can be shown that reciprocal points form a three dimensional lattice array. The trace of an (hkl) plane of the direct lattice intersects the c-axis, OC, at P (Fig 3). The intercept of the plane on the c-axis is $OP = \frac{C}{l}$, R is the corresponding reciprocal lattice point, and therefore $OR = \frac{1}{d_{hkl}}$. OD equals the spacing, d_{hkl}, of the planes. RN is constructed normal to OC. From[3] the triangle ODP :

$$\cos \rho = \frac{OD}{OP} = \frac{d_{hkl} l}{C}$$

From the triangle ORN

$$ON = OR \cos \rho = \frac{1}{d_{hkl}} \cos \rho$$

and therefore $ON = (\frac{1}{C})l$. Because the value of $\frac{1}{C}$ is a constant for a particular lattice, reciprocal points with identical l indices have the same value of ON. In other words, the points lie in planes that are normal to the c-axis and are spaced at interval of $\frac{1}{C}$. The value of ON is zero when $l = o$, hence the plane that contains the hko points - the hko level - passes through the origin of the

[3]E.W. Nuffield, X-Ray Diffraction Methods (New York: John Wiley and Sons, 1966) pp 239-248

direct lattice (Fig 4). The hk1 level of points is situated at a distance $\frac{1}{c}$ from the origin, measured along the c axis, the hk2 level is at $\frac{2}{c}$ and so on.

It can be similarly shown that the h0l, h1l, and h2l levels are normal to the b axis and spaced at interval of $\frac{1}{b}$, also that the 0kl, 1kl and 2kl levels are normal to the a axis and spaced at intervals of $\frac{1}{a}$

The reciprocal point 123 occurs in three levels: 1kl , h2l , and hk3. Consequently, it occurs at the intersection of these levels. Similarly, each reciprocal point is common to three levels. Therefore reciprocal points occur only at the level intersection and, because the levels are regularly spaced, the points form a three-dimensional lattice array.

Diffractions from Planes of Reciprocal Points

Figure 5 shows the sphere of reflection with OC, representing the c axis or [001] row of a crystal, oriented at an angle $\bar{\mu}$ to the beam. The hk0, hk1, hk$\bar{1}$, etc, levels of reciprocal point are normal to this row. They intersect the sphere in circles with diameters PQ, AB, DE, etc. The hk0 level includes the origin P of the reciprocal lattice. The Bragg condition is satisfied for any hk0 point, for example, which happens to be on the surface of the sphere, more particularly in this case on the circumference of the circle PQ. (The corresponding circles for the hk1 and hk$\bar{1}$

levels are AB and DE.) Because the reflections emanate from O and pass through these points, the reflections lie on a cone of which PQ is a right circular section. The cone is coaxial with OC. Reflections corresponding to hk1 and hk$\bar{1}$ points lie on coaxial cones with different half apex angles. The half apex angle of the zone level is equal to $\bar{\mu}$, but the angle for an n level depends on both $\bar{\mu}$ and the spacing of the reciprocal planes. Thus for the hk1 level:

$$\cos \bar{\nu} \quad = \quad \frac{OF}{OA} \quad = \quad OC + \frac{\lambda}{C}$$

$$OC \quad = \quad OP \cos \bar{\mu} \quad = \quad \cos \bar{\mu}$$

OA and O P = 1. Consequently

$$\cos \bar{\nu} \quad = \quad \cos \bar{\mu} + \frac{\lambda}{C}$$

It can be shown that for the hk$\bar{1}$ level

$$\cos \bar{\nu}' \quad = \quad \cos \bar{\mu} - \frac{\lambda}{C}$$

When rearranged into the form

$$C(\cos \bar{\nu} - \cos \bar{\mu}) \quad = \quad 1\lambda$$

$$C(\cos \bar{\nu}' - \cos \bar{\mu}) \quad = -1\lambda$$

the expression for diffraction from the two first-level reciprocal planes can be recognized as the Laue equations for first-order diffraction cones associated with the c axis of a crystal.

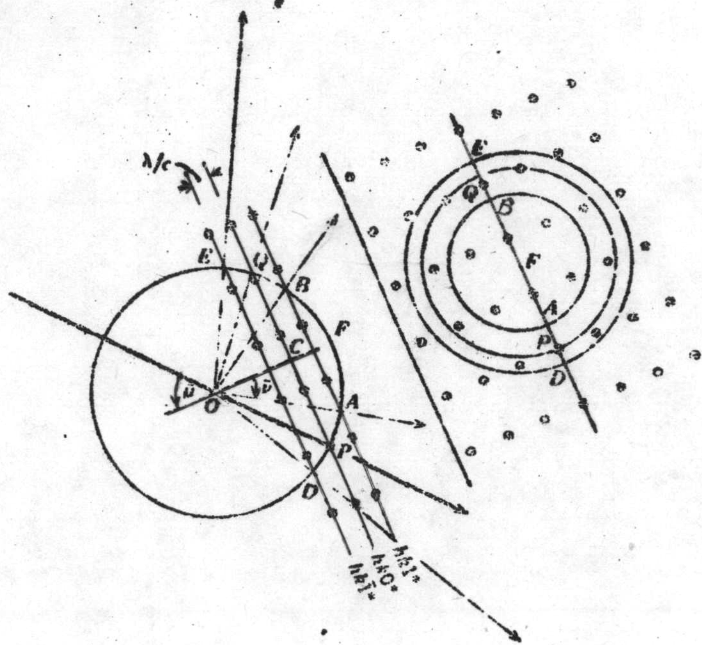

Fig. 5 Diffraction from planes of reciprocal points.

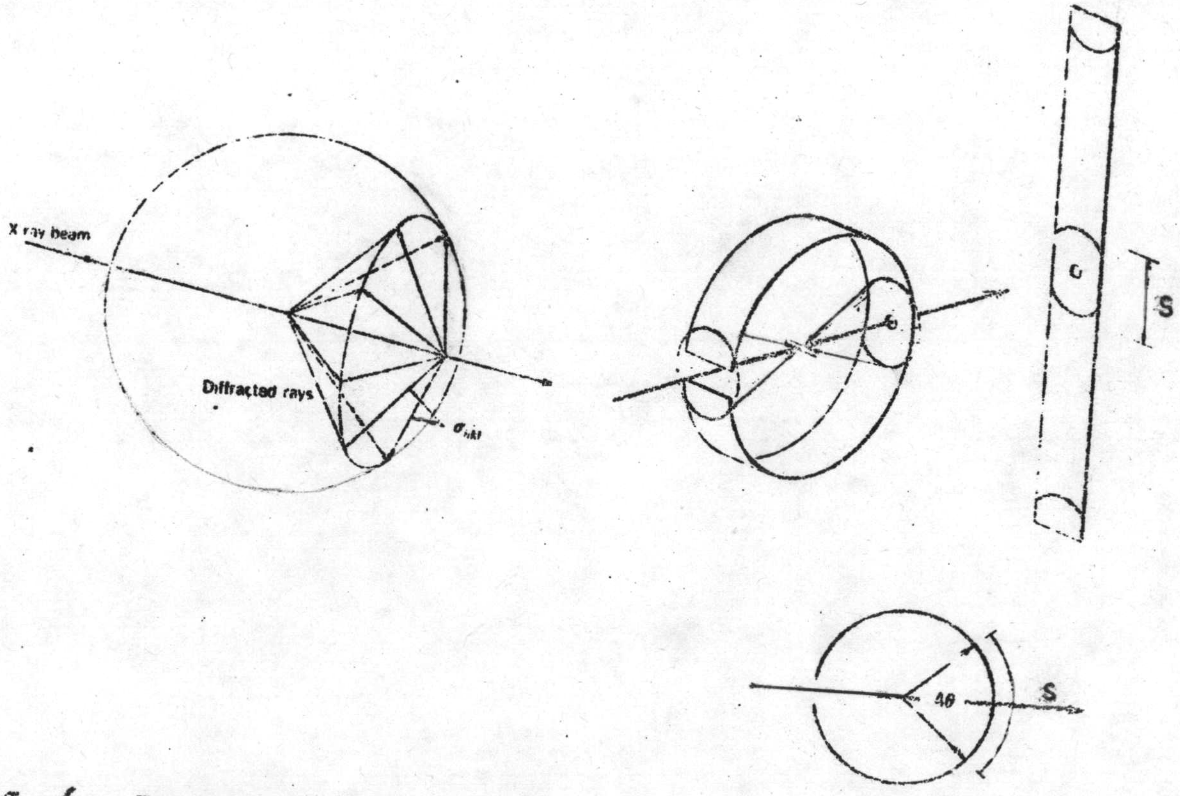

Fig. 6 Reciprocal lattice construction for one set of planes in a powder sample.

Fig. 7 The regular film position in a Debye-Scherrer camera.

2.2 The Powder Method

The essential features of the powder diffraction technique include a narrow beam of monochromatic x-rays impinging upon a crystalline powder composed of fine, randomly oriented particles. Ideally, all possible orientations of all possible lattice planes are present in a powder sample, and reflect x-rays when they are in position to satisfy Bragg reflection condition for x-rays of wavelength λ;

$$n\lambda = 2\,d\,\sin\theta \quad .$$

Each diffraction line is made up of a large number of small spots, the spots lying so close together that they appear as a continuous line. The lines are generally curved, unless they occur exactly at $2\theta = 90^{\circ}$ when they will be straight.

Consider[4] just one reciprocal lattice vector, $\vec{\sigma}_{hkl}$; if the number of crystallites present in the powder is very large and the crystallites are randomly oriented, such reciprocal lattice vectors in each crystallite point in all possible directions, so that the corresponding reciprocal-lattice points lie on the surface of a sphere of radius $|\vec{\sigma}_{hkl}|$. Obviously, a separate sphere exists for each conceivable value of σ_{hkl}, so that the reciprocal lattice of a powder is, simply, a set of concentric spheres. Since the origin of the reciprocal lattice of each crystallite must lie at the point of emergence

---

[4] L.V.Azaroff, Elements of X-Ray Crystallography (New York: Mc Graw-Hill, 1968) pp 152-153.

of the incident x-ray beam, each reciprocal-lattice sphere cuts the sphere of reflection, provided that $\sigma_{hkl} < \frac{2}{\lambda}$ (Fig. 6). Since the distribution of reciprocal-lattice points along the surface of the sphere is uniform for a truly random polycrystalline aggregate, the distribution of the x-rays along the diffraction cone is also uniform, so that it is sufficient to intercept a representative portion of each cone.

The Debye-Scherrer Method

A number of methods are employed to record powder x-ray reflections on film. Each is designed to exploit particular applications. The so called Debye-Scherrer technique has proved to be the most useful for the routine identification of unknown compounds. Furthermore, it is capable of yielding lattice spacings of high precision. The Debye-Scherrer method makes use of a cylindrical film, whose axis coincides with the rotation axis of the sample and is normal to the beam. Each reflection cone intersects the film in a pair of arcs, and all the cones generated by the specimen are represented on the film. The distance S (Fig. 7) between a pair of arcs on the film bears a simple relation to the apex angle 4 θ of the corresponding reflection cone.

$$S/R = 4\theta$$

$$\theta = (1/4R)S \quad \text{radian}$$

$$\theta = (180/4\pi R)S \text{ degree}$$

where R is the radius of the film.

Focusing Camera

The main disadvantage with Debye-Scherrer cameras is that the absorption of x-rays by the specimen causes the lines to be displaced from the true positions in a direction of increasing Bragg angle. This effect is largest and therefore most serious at the low angle end of the pattern, which incidentally is the all-important region for indexing powder data. Absorption effects can be partially overcome by incorporating a standard substance with the material under examination and so be able to draw up a correction curve. Focusing cameras fall into two categories.

1) Those which use the x-ray beam direct from the tube.
2) Those which use from a focusing monochromator.

Focusing Camera Used Without a Focusing Monochromator

The principle of the focusing camera is illustrated in Fig.8. The specimen is in the form of a thin layer of powder, MM' Three or four centimeters long, lying on the circumference of a circle, and the x-ray film, CD, also lies on this circle. The slit, S, allows a divergent beam of x-rays to fall onto the powder specimen. P is the focus of a typical reflected ray. The conditions for focusing and reflecting

depend solely on the geometry of the camera. Thus let N be the mid-point of the arc SP. Then $S\hat{M}N = S\hat{M}'N = N\hat{M}P = N\hat{M}'P$ (angles subtended by equal arcs). Any lines which bisect the angles subtended by the arc SP will therefore intersect at the point N. Let the incident ray SM make an angle $\pi/2 - \theta$ with the line NM. This would be the condition for reflection for a crystal plane normal to the line NM. The reflected rays will be generated and come to a focus on the same circumference as the slit, S, provided the lattice planes are tangential to the circumference of a cylinder of radius NM and touch the circumference of the camera cylinder of radius r.

<u>Focusing Cameras Used with a Focusing Monochromator</u>

The chief advantages of these cameras are that photographs taken with them have little background fog, owing to the almost complete elimination of white radiation, and the lines are not displaced by absorption of the x-rays in the specimen. Their chief disadvantage, as with all focusing types, is that a number of cameras are needed to cover the range of 0 to 90° of Bragg angle, but experience has shown that a camera covering the range of 0 - 40° of Bragg angle will serve most purposes. The exception is when orders of accuracy higher than $\pm$ 0.02 percent are required.

<u>The Guinier-type focusing camera</u>

It is well known that the Guinier Method of obtaining monochromatic x-ray powder diffraction photograph has the

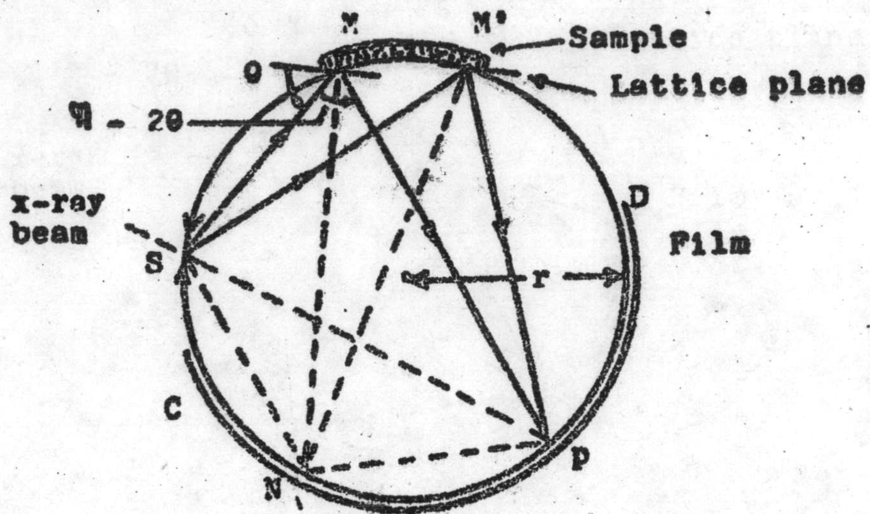

Fig. 8 The essential features of focusing camera.

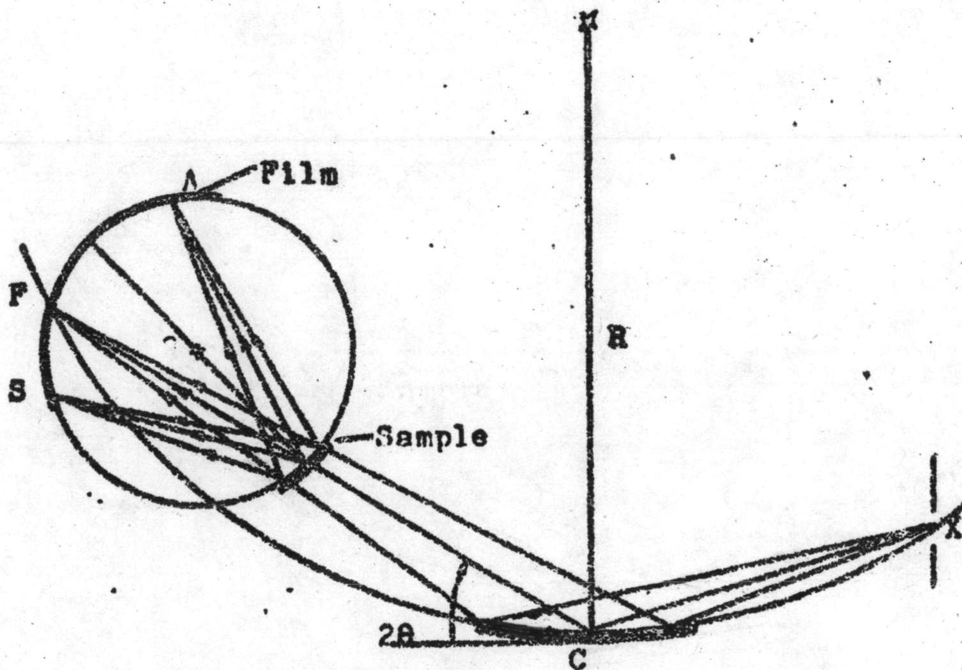

Fig. 9 Diagrams showing the principle of the Guinier method.

advantage of giving a very high resolution and an extremly low background, the exposure time is very short and the amount of specimen required is extremely small.

The principle of Guinier method is illustrated in the schematic drawing in Fig. 9. The camera uses monochromators of Johansson type with a cylindrically ground and bent quartz crytal reflecting from the plane (10$\bar{1}$1). The choice of the radius of curvature is governed by the elastic properties of quartz and the distance needed between the monochromator and the focal line of the radiation. When possible, the radius of curvature should vary with the wavelength so that this distance remains nearly constant. This can be achieved for CuKα, FeKα, and CrKα radiation but not for MoKα. The first three require radii of the order 600 and 300 mm, whereas the last needs 600 and 1200 mm. Quartz has been chosen as crystal material because of its excellent focussing properties together with its relaive-ly low price. The camera is normally intend to work in vacuum with Cr-radiation, this is necessary in order to reduce air absorption. Evacuation also reduces scattering from the air in the path of the primary beam. The vacuum chamber encloses the monochromator. The exposure time is also reduce because of the shorter path of the x-rays in air, which is especially important when Cr-radiation is used.

005872

117998967

From Fig.9 , a converging x-ray beam, produced by reflecting the incident beam from a curved crystal monochromator, is transmitted through the specimen, the deviation angle 2Θ at the monochromator has a definite and accurately known value for a given wavelength. The central primary beam x C is taken out at an angle of 4.5° to the target plane of the x-ray tube. According to the radiation to be used the combined specimen holder, film holder system is set at the corresponding 2Θ angle and is then translated along the direction CF so that the line focus F falls on the film.

Film measurement and calculation of Bragg-Angles

The usual way of deriving Θ is to measure the distance between the primary and diffraction lines, SS_o (Fig 10). The distance SS_o of each diffraction line on the film bears a simple relation to the apex angle $4\,\Theta$ of the corresponding reflection cone.

$$4\,\Theta \text{ (radian)} = (S-S_o)/R$$

$$\Theta \text{ (degree)} = \frac{180}{\pi}\,\frac{S-S_o}{4\,R} = K(S-S_o)$$

where $K = 180/4\pi R$ and $K = \Theta/S-S_o$,

R is the radius of the film.

When a camera whose radius is a multiple of $180/\pi = 57.3$, it is possible to measure the diffraction angle directly with a millimeter scale, and lead to a solution of Bragg's equation for the value of the spacing d ($d_{hkl} = \frac{\lambda}{2\sin\Theta_{hkl}}$).

Several precautions are necessary in determining the line position. The film should be adjusted so that its length is parallel to the direction of travel of the microscope. The position of the line should be read by placing the diagonal cross wire on the middle of the arc ; two or three readings should be taken. The visibility of weak lines is also improved by putting opaque screens over that part of the film which has not received any radiation, so that only the exposed part is visible. The eye has then to accommodate itself to only a small range of brightness.

Analytical Methods for Indexing

Following the determination of the d value from a powder photograph, it is frequently desired to identify the corresponding crystallographic planes(hkl). Ito's method is one procedure for indexing the reflections of a powder pattern regardless of symmetry. This method is based on the fact that each reflection of a powder photograph corresponds to a vector in reciprocal space. If three noncoplanar vectors are selected, the edges of a unit cell are defined, and if three more are selected, their interaxial angles are fixed. This corresponds to the selection of six appropriate lines on the powder photograph. Once an appropriate unit cell is selected, it becomes possible to index all the lines on the powder photograph. The

expression relating the reciprocal-lattice vector, $\vec{\sigma}_{hkl}$, to the reciprocal-cell dimensions of a triclinic cell is

$$\sigma^2_{hkl} = d^{*2}_{hkl}$$

$$= h^2a^{*2}+k^2b^{*2}+l^2c^{*2}+2hka^*b^*\cos\gamma^*+2klb^*c^*\cos\alpha^* +2lhc^*a^*\cos\beta^*$$

let $\quad q_{hkl} = \sigma^2_{hkl}$

If the first three lines at the low angle end of the pattern are taken to have indices 100, 010 and 001 then a^*, b^* and c^* can be derived from the following equations:

$$q_{100} = a^{*2},\ q_{010} = b^{*2},\ q_{001} = c^{*2}$$

The values for the reciprocal cell angles α^*, β^* and γ^* have now to be found. Fig.11 shows the planes of the reciprocal lattice containing the vectors b^* and c^*. The length of the vector $\vec{\sigma}_{okl}$ is given by

$$q_{okl} = k^2b^{*2}+ l^2c^{*2}+ 2klb^*c^*\cos\alpha^*$$

Similarly

$$q_{ok\bar{l}} = k^2b^{*2}+ l^2c^{*2}- 2klb^*c^*\cos\alpha^*$$

If these two equations are added and subtracted, there results adding :

$$q_{okl} + q_{ok\bar{l}} = 2k^2b^{*2}+ 2l^2c^{*2}$$

subtracted :

$$q_{okl} - q_{ok\bar{l}} = 4\ kl\ b^*c^*\ \cos\alpha^*$$

The last relation can be solved for $\cos\alpha^*$

[library stamp]

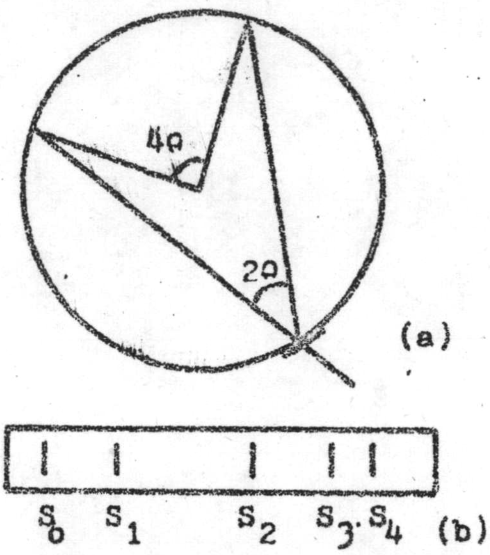

Fig.10 The regular film position in a Guinier-Hagg Powder camera.

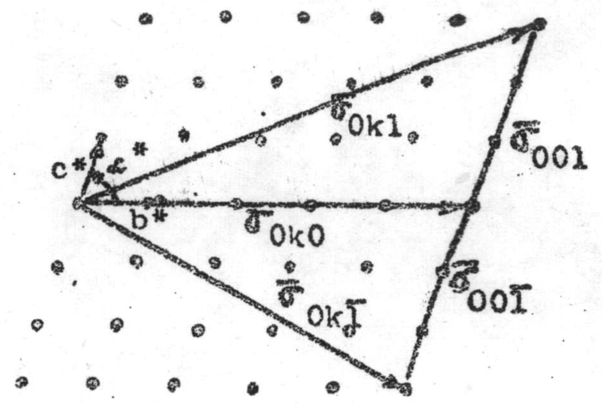

Fig.11 The reciprocal lattice plane containing the vector b* and c*.

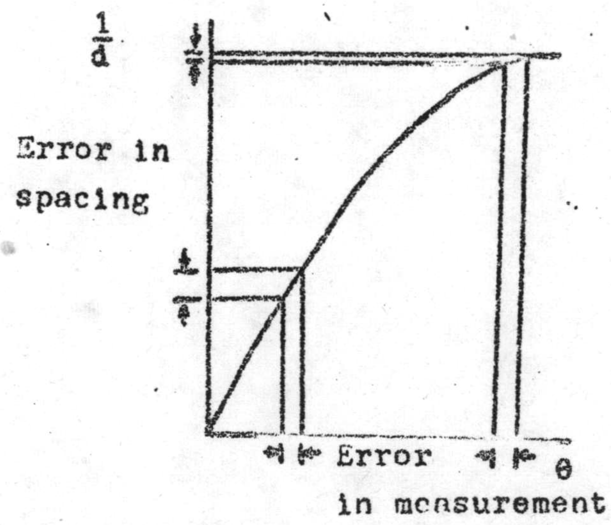

Fig.12 The relation between the Bragg angle θ and the spacing d.

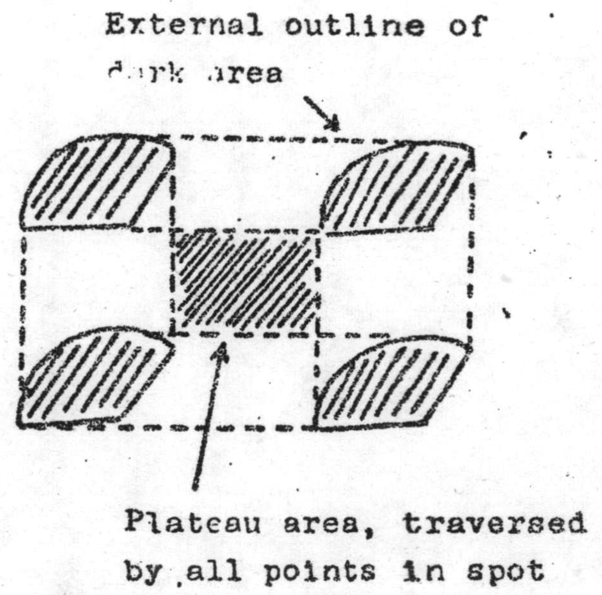

Fig. 14 Reflection spot.

$$\cos\alpha^* = \frac{q_{okl} - q_{ok\bar{l}}}{4\,kl\,b^*c^*}$$

The other two angles β^* and γ^* are derived in the same way. To solve α^*, one must first search among the q's to find two whose average value is $k^2b^{*2} + l^2c^{*2}$. For example, if the reflections 011 and $01\bar{1}$ are not absent, then the average value of these q's is $b^{*2} + c^{*2}$. If symmetrically placed quantities cannot be found, it may mean that one of the pair, for example the 011 line is missing. In this case the next step is to look for symmetrically placed quantities about the quantity $4b^{*2}+c^{*2}$ or $b^{*2}+4c^{*2}$, which if successful would locate the pairs of planes 021, $02\bar{1}$, or 012, $01\bar{2}$. On the other hand it may mean that the first three reflections on the pattern are not all first order reflections. In this case, other indices hoo, oko, ool should be assigned to them and the search for pairs of lines repeated. If again no pairs of lines can be found, assign the indices hoo, oko and ool to another group of three lines. When symmetrical pairs of lines have been located and the angles α^*, β^* and γ^* calculated, all possible q values are calculated and compared with the observed values. If the comparison is acceptable this test is sufficient to prove the correctness of the assigned reciprocal lattice.

<u>The derivative of accurate unit cell dimensions</u>.

The accuracy of the unit cell dimensions determined by the method discussed above is seldom better than ± 0.1 percent. Unfortunately various systematic and subjective errors which

occur in the process of obtaining and measuring an x-ray powder diffraction photograph often make these high orders of accuracy difficult to attain. Errors in the value ascribed to θ , the Bragg angle, affect that of the cell constant derived from it. These errors and methods by which they can be reduced can be discussed under the two heading subjective and systematic.

<u>Subjective errors</u>

All measurements of the films should be checked so that errors arising from an incorrect vernier reading or a mis-set cross hair are avoided. This is so important as to make it well worth while to take a number of independent measurements on each line, preferably allowing the cross hair to approach the line alternatively from either side.

<u>Systematic errors</u>

The data from which cell constants are derived depend upon the recognition of peak position of arcs on a diffraction photograph. Since these peak positions depend on the experimental conditions discussed below , it is easy for systematic errors to appear in the values of the cell constants.

The curves of Fig.12 indicate that for a given precision in measuring θ the error in d, hence in the cell edge a, decreases as θ increases. This can also be shown analytically by differentiating the Bragg equation with respect to θ .

$$n\lambda = 2d \sin\theta$$

$$0 = 2\frac{\Delta d}{\Delta\theta}\sin\theta + 2d\cos\theta$$

$$\frac{\Delta d}{d} = \frac{-\cos\theta}{\sin\theta}\Delta\theta = -\cot\theta\,\Delta\theta$$

As θ increases to 90°, $\cot\theta$ approaches zero and the error $\Delta\theta$ produces ever smaller errors Δd in measured d. Hence the desirability where possible of using a camera which allows the recording of reflections at high values of θ.

The experimental condition which will affect the position of an arc on a diffraction photograph when this type of camera is employed is film shrinkage. There are three general methods for overcoming this difficulty:

a) to print fiducial marks on the film before processing,

b) to print a complete scale on the film before processing,

c) to mix the unknown substance with a standard substance which then gives diffraction arcs at accurately known angles.

To eliminate systematic errors by the use of an internal calibration standard, a standard cubic substance, in the form of a powder, is mixed with the material under investigation, and in this way diffraction pattern of both are obtained on the same film under identical experimental conditions. The standard material should be chosen so that its diffractions pattern does not mask any of the lines of the specimen itself. Then provided the refraction correction is taken into account and the specimen and standard are of comparable crystallite size, preferably between 1 and 0.1μ, then the effect of systematic errors will be the same for both substances. The cell parameter of the standard being

known, the $\theta/S-S_o$ values is plotted against the corresponding value of the $S-S_o$. From measuring all diffraction line positions S, the $S-S_o$ values are obtained. Interpolating and extrapolating from the graph the $\theta/s-s_o$ are determined, and then θ. The graph gives the correction factor to be applied for any value of $\sin^2\theta_{obs}$. The $\sin^2\theta_{obs}$ values for the material under investigation are now corrected, using the graph to obtain the correct fraction for each reflection. From the corrected values of $\sin^2\theta$ the true value of the cell constant is obtained.

2.3 Intensity Measurement

The Rotation and Weissenberg photograph are taken by the methods discussed elsewhere.[5] The Weissenberg arrangement is the commonly used method for recording diffraction intensities photographically. Assuming that the crystal being photographed is smaller than the incident beam's cross-section, the size and shape of each reflection are proportional to that of the crystal. Because the final film is viewed with visible light, it is convenient to define density D or blackening B in terms of this light. This is defined as

$$B = D = \log I_o/I$$

where I_o and I are, respectively, the intensities of light incident upon and transmitted through the film.

---

[5] W. Chaipayungpun, Preliminary X-ray Crystallographic Study of Certain Chemical Constituents of Stemona Roots, (Thesis Graduate School, Chulalongkorn University, 1970)

Intensity measurement may be carried out by either of two different kinds of instrumentation, the photographic film or the quantum counter. With either of these devices it is possible to measure the intensity.

Fig.13 is a graph of the blackening curve, versus the number of times through the reflection angle, n. I is the degree of blackening of a reflection spot and I_o is the background blackness surrounding the spot. The graph is derived as follows: An approximation scale, obtained by passing a crystal on a Weissenberg camera an increasing number (n) of times through a given reflection angle, is used to determine the I_o/I_n ratio of all reflection spots, and D, the decimally based logarithm of this ratio ($\log_{10} I_o/I_N$) is then plotted against the number (n) of crystal reflection cycles. The intensities of each reflection were measured by using a microdensitometer. The degree of blackening, I, of a reflection spot is measured and immediately afterwards the background blackness (I_o) surrounding the spot. From the value of the ratio I_o/I the degree of intensity can be determined by using the graph.

Multiple-film technique

To the eye, a blackening of two (B = 2) appears very dark and constitutes an upper limit of observation. The doubly coated film normally used, however is capable of

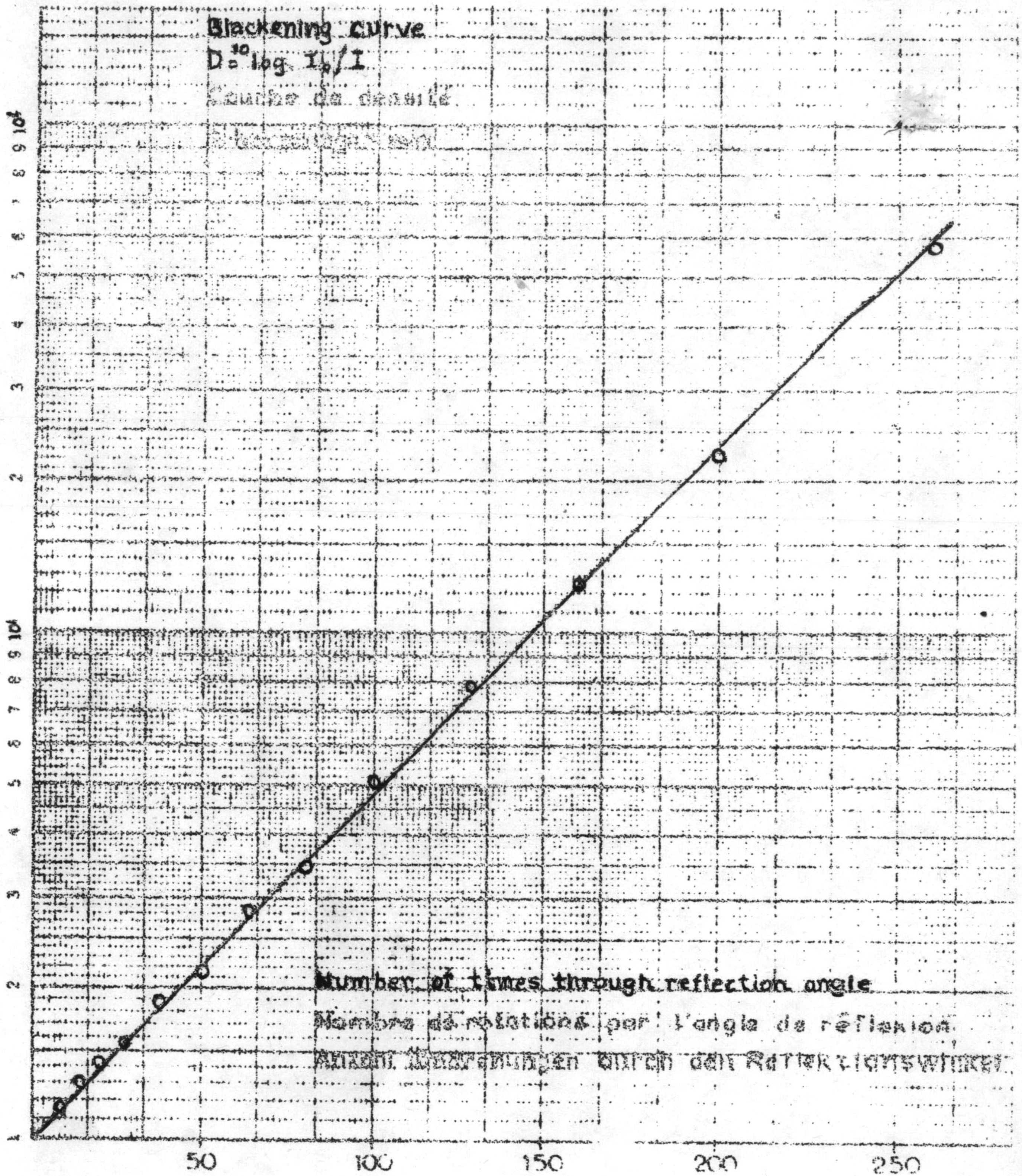

Fig. 13 Blackening curve

recording blackening up to B =3. To overcome this limitation, the camera is loaded with several superposed films. Hence the x-rays that strike the second film have gone through the first film and are thereby reduced in intensity. In like manner, the x-rays striking the third film have passed through the first and second films. In this way the weaker maxima may give the correct exposure to the first film while the strongest maxima may be reduced by the time they get to the third film to give it about the correct exposure. While the multiple-film technique is ordinarily used for measuring peak intensities, it may also be used for measuring integrated intensities by various methods.

Integrated-intensity methods

Integrated intensities are more difficult to determine than peak intensities because the x-ray spot is blacker in the central region and lighter toward the edge. Each region of the spot has thus received different intensities. Each of these intensities must be added to make up the total integrated intensity. The chief difficulty in doing this is that intensity cannot be measured directly but is ordinarily arrived at by measuring the light transmission of the blackened photographic film. Unfortunately this is not a linear function of the intensity received by the region. Thus it is not possible to simply add together the light transmitted through the several regions of the spot. One of the methods to circumvent this difficulty is the plateau method. A Weissenberg apparatus in which the cylindrical camera undergoes a slight rotation about the axis of

the cylinder and also a small auxiliary translation parallel to the axis of the cylinder was used. The rotation is caused by the slating level, which pushes on the horizontal lug attached to the camera. The ratchet is about to be rotated as the lower-left pin engages the stationary pin. The spring and the ball-bearing disk at the left of the ratchet fix the position of the ratchet in one of 14 positions. Fig. 14 shows how the position of the x-ray spot migrates over a small area of the film with this arrangement. The plateau region is the shaded portion in the center of the migration area. Within this region the film has received contributions from all parts of the migrating spot. Since the optical density of the multiply exposed region is directly proportional to the integrated intensity, a microdensitometer can be used to measure the intensity of each reflection. The chief limitation of this arrangement is the accumulation of background intensity during the necessarily prolonged exposure.

2.4 Refinement of Unit Cell Dimensions

The Method of Least Squares

A analytical method of refinement of great power and generality is that based on the principle of least squares. Consider a linear function with n variables $x_1, x_2, \ldots, x_n$. These variables can be thought of as defining a space whose value at any point is determined both by the location $x_1, x_2, \ldots, x_n$ and by independent parameters $P_1, P_2, \ldots, P_n$ which define the function.

Thus

$$f = P_1x_1 + P_2x_2 + P_3x_3 + \dots + P_nx_n \quad \dots\dots(1)$$

If the values of the function are measured at m different points with $m > n$, the principle of least squares states that the best values for the parameters $P_1, P_2, \dots, P_n$ are those which minimize the sums of the squares of the properly weighed difference between the observed and calculated values of the function for all the observational points. Thus the quantity to be minimized is given by

$$D = \sum_{r=1}^{m} w_r(f_{o_r} - f_{c_r})^2 \quad \dots\dots(2)$$

where w_r is the weight to be assigned an observation, f_{o_r} is one of the m observed values of the function, and f_{c_r} is the corresponding calculated value. To obtain the best fit, it will be necessary to consider the parameters P as variables which may be adjusted to minimize D. This is a straightforward minimization problem which is treated by differentiating equation (2) with respect to each of the parameters in turn and setting the derivative equal to zero.

This gives

$$\sum_{r=1}^{m} w_r(f_{o_r} - f_{c_r}) \frac{\partial f_{c_r}}{\partial P_j} = 0 \quad (j=1,2,\dots,n) \quad \dots\dots(3)$$

a set of n equations in n unknowns called the normal equations. In practice, there are m observational equations of the form

of eq(1), one for each observation. Since we shall be treating each parameter P_j as a quantity to be adjusted, and the x's have different fixed values for each of the m observations, it is customary to reverse their order. Taking the partial derivatives $\frac{\partial f_{c_r}}{\partial P_j}$ for each of the m observational equations and substituting in eq.(3) gives the n normal equations.

$$\sum_{r=1}^{m} w_r(f_{o_r} - x_{r1}P_1 - x_{r2}P_2 - \ldots - x_{rn}P_n)x_{r1} = 0$$

$$\sum_{r=1}^{m} w_r(f_{o_r} - x_{r1}P_1 - x_{r2}P_2 - \ldots - x_{rn}P_n)x_{r2} = 0 \qquad (4)$$

$$\vdots$$

$$\sum_{r=1}^{m} w_r(f_{o_r} - x_{r1}P_1 - x_{r2}P_2 - \ldots - x_{rn}P_n)x_{rn} = 0$$

Rearranging and writing more fully,

$$\sum_{r=1}^{m} w_r x_{r1}^2 P_1 + \sum_{r=1}^{m} w_r x_{r1} x_{r2} P_2 + \ldots + \sum_{r=1}^{m} w_r x_{r1} x_{rn} P_n = \sum_{r=1}^{m} w_r f_{o_r} x_{r1}$$

$$\sum_{r=1}^{m} w_r x_{r2} x_{r1} P_1 + \sum_{r=1}^{m} w_r x_{r2}^2 P_2 + \ldots + \sum_{r=1}^{m} w_r x_{r2} x_{rn} P_n = \sum_{r=1}^{m} w_r f_{o_r} x_{r2}$$

$$\vdots$$

$$\sum_{r=1}^{m} w_r x_{rn} x_{r1} P_1 + \sum_{r=1}^{m} w_r x_{rn} x_{r2} P_2 + \ldots + \sum_{r=1}^{m} w_r x_{rn}^2 P_n = \sum_{r=1}^{m} w_r f_{o_r} x_{rn}$$

Solution of these n equations gives directly the best values of the parameters P_j in the least-squares sense.

2.5 The Crystal Structure Factor.

The crystal structure could be found from diffraction spectra. The structure can be determined from a knowledge of the intensities and phases of the diffraction spectra. The experimental part of a crystal-structure analysis consists in the gathering of accurate values of the intensities of the many spectra which is discussed in 2.3. It is most convenient to work with a set of amplitudes, $|F_{hkl}|$, of the spectra rather than the intensities themselves. This requires the conversion of intensities to amplitudes for all spectra. Unfortunately the "integrated intensities" derived from the experiment are not merely the squares of the corresponding amplitudes. They contain several factors which must be allowed for. The transformed equation is

$$|F_{hkl}|^2 = K \frac{1}{L_{hkl} P_{hkl}} I_{hkl}$$

The scale factor, K, may be neglected since I_{hkl} is ordinarily not measured in absolute units anyway. The Lorentz factor, L_{hkl}, and the polarization factor, P_{hkl}, differ from reflection to reflection. Thus each relative intensities, I_{hkl}, must be multiplied by 1/LP to obtain a set of $|F_{hkl}|$'s.

Polarization Factor

The characteristic radiation obtained from a diffraction tube is generally considered to be unpolarized. However, the process of scattering causes the diffracted beams to be partially polarized, the amount of polarization depend on the

angle of scattering. The polarization factor is a simple function of 2θ, and is given by

$$P = \tfrac{1}{2}(1 + \cos^2 2\theta).$$

<u>Lorentz Factor</u>

The Lorentz factor is concerned with the specific motion of the crystal. In most single-crystal x-ray methods the specimen is given a controlled motion in the path of the x-ray beam. Various planes n the crystal are thereby succesively presented to the beam at their respective Bragg angles and are given an opportunity to reflect. The rate at which the planes pass through the Bragg condition varies with the diffraction angle, and therefore each intensity measurement must be separately corrected for the time that a particular plane depends in rotating through the Bragg angle. The form of this correction, which is known as the Lorentz factor, depends on the method of recording the reflections.

Assume that the crystal is rotating with a constant angular velocity w about an axis normal to the page at R (Fig. 15). The Bragg condition for the planes is satisfied, and the planes reflect during the time that it takes P to cross the circumference of the circle. The time involved depends on the velocity of P

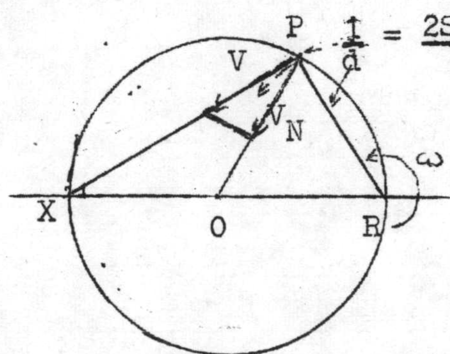

Fig. 15 The Lorentz factor for reflection in the plane of the page.

and the angle at which the point intersects the circle on the velocity component V_N normal to the circumference of the circle. Points far from R move more rapidly than those near R, but pass through the circle at more oblique angles. The velocity V of the point is $RPw = (1/d)w = (2 \sin \theta/\lambda)w$ and at P is directed along PX. The velocity component normal to the circle has the direction PO, at an angle θ to PX. Therefore

$$V_N = V \cos \theta = (\frac{2 \text{ son } \theta}{\lambda} w) \cos \theta = \frac{\sin 2\theta}{\lambda} w.$$

If E is the total energy of radiation reflected by a set of planes in the time that it takes P to cross the circumference of the circle

$$E\, V_N = Ew(\frac{\sin 2\theta}{\lambda}) = I_C$$

where I_C is the intensity of scattering by the crystal. The product $Ew(\sin 2\theta/\lambda)$ is constant for a given beam intensity. The relation can usefully be recast to give energy in terms of the angular velocity of the crystal.

$$Ew = I_C\, (\lambda/\sin 2\theta)\ .$$

Because energy is intensity multiplied by time, the quantity $(\lambda/\sin 2\theta)$ express the time that the planes spend in reflecting energy E. Hence $(1/\sin 2\theta)$ express the relative tive that any crystal plane spends in rotating through the small angular range of θ over which reflection occurs. This quantity is known as the Lorentz factor. The factor evidently has a different form for reflection planes which are not parallel

to the rotation axis. The Lorentz Factor for the zero level of a rotation crystal photograph and for the upper level is

$$L = 1/2((1-\sin^2\theta)(\sin^2\theta-\sin^2\mu))^{\frac{1}{2}}$$

where μ = equi-inclination angle and

θ = Bragg angle

$$\sin^2\mu = \frac{n^2\lambda^2}{4c^2}$$

C = the length of rotational axis in Å

n = the number of layer

$$\sin^2\theta = \frac{\lambda^2}{4d^2_{hkl}}$$

d = interplanar spacing.

For triclinic system

$$d^2 = \left[\frac{\frac{h^2}{a^2}\sin^2\alpha + \frac{k^2}{b^2}\sin^2\beta + \frac{l^2}{c^2}\sin^2\gamma + \frac{2hk}{ab}(\cos\alpha\cos\beta - \cos\gamma) + \frac{2kl}{bc}(\cos\beta\cos\gamma - \cos\alpha) + \frac{2lh}{ca}(\cos\gamma\cos\alpha - \cos\beta)}{1 - \cos^2\alpha - \cos^2\beta - \cos^2\gamma + 2\cos\alpha\cos\beta\cos\gamma}\right]$$

From the above equation, it is obvious that the Lorentz factors for the upper levels are larger than that for the lower level, and the Lorentz factors for the Zero level is (1/sin 2θ).